

Analysis of Numerical Seismic Source Functions by Finite Difference Method

Shujaat Ali¹, Mubarik Ali¹ and Ahmad Naveed²

ABSTRACT

The finite difference synthetic seismograms are tested for a number of seismic sources to understand their stability characteristics. Processing techniques such as frequency filtering and gain application are applied to improve the model response. The grid dispersion due to high frequencies contained in source appears to be controllable by high cut filtering the model output. A single velocity distribution model is used to prepare synthetic seismograms with different source functions. The results seem to be in agreement with the previous work. The output of modeling algorithm gives correct arrival times but when the model becomes unstable, the relative amplitude information of different arrivals seems to be lost. The use of different seismic source wavelets with same central frequency indicates that model stability and numerical anisotropy also depend on the pulse shape or phase characteristics of the source. From the present study it is concluded that in addition to previous work, which showed the numerical stability a frequency dependent phenomenon, it also depends on the phase spectrum of the input source wavelet.

INTRODUCTION

A number of methods are available for forward modeling such as ray tracing, normal incidence, etc., but numerical methods based on heterogeneous elastic wave equation are of special value. Except for the contributions due to inelastic behavior of earth, they account for all phenomena associated with seismic wave propagation such as multiple reflections, surface waves (ground roll), shear and converted wave.

In past the biggest drawback of these scheme was the immense speed and huge computer memory required by these schemes. The increased efficiency of modern computers has imposed new emphases on the application of numerical methods to forward modeling for the models with dimensions of geological interest.

Any numerical scheme for the solution of a continuous field problem is valid only if the deviation between analytical and numerical results is small. The synthetic seismograms based upon the finite difference formulations may contain several of such effects, such as grid dispersion (Kelly et al., 1976), numerical anisotropy and model truncation related boundary or edge reflections.

Waves traveling on a discrete grid become progressively dispersed with increasing travelttime. The phenomenon

known as grid dispersion is studied in detail by Alford et al. (1974), who have compared the synthetic seismograms computed for the simple models by homogeneous approximation finite difference and by analytical solutions founded by using the Eigen function expression technique. Their results show that the grid dispersion increases with the increase in the ratio between wavelength of signal in the medium and spatial grid interval. Grid dispersion produces a normal variation of velocity with frequency, i.e. the higher frequencies are delayed related to the lower signal frequencies and "tailing" of the signal arises. As a rule of thumb, the number of grid points per wavelength at upper half power frequency of the source should be approximately ten or more.

The model prepared by finite difference solution of the wave equation is limited in terms of grid points by the available computer memory. This restriction introduced artificial boundaries, which produce undesired edge reflections. There are new schemes made available recently. One such method is the replacement of the boundaries by the absorbing conditions (Randall, 1988; Huato and Lees, 1997; Fornberg, 1988) having viscous behavior.

As the edge reflections have the characteristic moveouts, they can be eliminated by the migration in frequency wave number domain as well.

The errors related with Finite Difference Method (FDM) formulation of the elastic wave propagation problem as described by Wild (1998) can be divided into three types: first are the errors related with the linear drift that may vary in magnitude from time to time and may also change its sign during this. Second is numerical anisotropy related with the anisotropic behavior of formulation while dealing with more than one dimension even if the model is isotropic and homogeneous. Third are most serious and are known as the Neumann instability errors, these errors not only propagate through a grid but their magnitude also increases exponentially with iterations.

Along with these errors, Seron et al. (1996) have also described errors such as numerical polarization that are related with propagation of longitudinally or transversely polarized waves.

WAVE PROPAGATION PROBLEM IN TWO DIMENSIONAL HETEROGENEOUS MEDIA

The heterogeneous formulation of wave equation allows spatial variations in the material properties. In the heterogeneous formulation, Lamé constants $\lambda(m, n)$, $\mu(m, n)$ (where m and n are discrete spatial coordinates) need not to be constant for a single medium but may have even grid point to grid point variation. The scheme accounts

¹ Department of Earth Sciences, Quaid-i-Azam University, Islamabad.

² Premier Shell BV, Islamabad.

automatically for the spatial variation in the elastic parameters across an interface whose geometrical complexity is limited only by the choice of the grid intervals Δx , and Δz . The boundary conditions in heterogeneous formulation are implicitly defined.

The following equation describes the propagation of elastic waves in 2D heterogeneous medium,

$$\rho \frac{\partial^2 u}{\partial t^2} = \frac{\partial}{\partial x} \left\{ \lambda \left(\frac{\partial u}{\partial x} + \frac{\partial w}{\partial z} \right) + 2\mu \left(\frac{\partial u}{\partial x} \right) \right\} + \frac{\partial}{\partial z} \left\{ \mu \left(\frac{\partial w}{\partial x} + \frac{\partial u}{\partial z} \right) \right\} \quad (1)$$

$$\rho \frac{\partial^2 w}{\partial t^2} = \frac{\partial}{\partial z} \left\{ \lambda \left(\frac{\partial u}{\partial x} + \frac{\partial w}{\partial z} \right) + 2\mu \left(\frac{\partial w}{\partial z} \right) \right\} + \frac{\partial}{\partial x} \left\{ \mu \left(\frac{\partial w}{\partial x} + \frac{\partial u}{\partial z} \right) \right\}$$

The assumption that density ρ is constant throughout the model enables us to write above equation as a function of the spatially varying P and SV wave velocities. The Lamé constants can be replaced by expressions in terms of SV and P- waves velocities and after the conversion of the above equation into a set of finite difference explicit solution one gets the following results,

$$\begin{aligned} \frac{u(m, n, l+1)}{\Delta t^2} &= \frac{2u(m, n, l) - u(m, n, l-1)}{\Delta t^2} + \frac{1}{\Delta x} \left\{ \left[\frac{\alpha^2(m+1, n) + \alpha^2(m, n)}{2} \right] \left[\frac{u(m+1, n, l) - w(m, n, l)}{\Delta x} \right] \right. \\ &\quad - \left. \left[\frac{\alpha^2(m, n) + \alpha^2(m-1, n)}{2} \right] \left[\frac{u(m, n, l) - u(m-1, n, l)}{\Delta x} \right] \right\} + \frac{1}{2\Delta x} \{ \alpha^2(m+1, n) \\ &\quad \left[\frac{u(m+1, n+1, l) - u(m+1, n-1, l)}{2\Delta z} \right] - \alpha^2(m-1, n) \left[\frac{u(m-1, n+1, l) - u(m-1, n-1, l)}{2\Delta z} \right] \} \\ &\quad + \frac{2}{2\Delta x} \{ \beta^2(m+1, n) \left[\frac{w(m+1, n+1, l) - u(m+1, n-1, l)}{2\Delta z} \right] - \beta^2(m-1, n) \\ &\quad \left[\frac{w(m-1, n+1, l) - w(m-1, n-1, l)}{2\Delta z} \right] \} + \frac{1}{2\Delta z} \{ \beta^2(m, n+1) \left[\frac{w(m+1, n+1) - w(m-1, n+1, l)}{2\Delta x} \right] \right. \\ &\quad - \left. \beta^2(m, n-1) \left[\frac{w(m+1, n-1, l) - w(m-1, n-1, l)}{2\Delta x} \right] \} + \frac{1}{\Delta z} \left\{ \left[\frac{\beta^2(m, n+1) + \beta^2(m, n)}{2} \right] \right. \\ &\quad \left. \left[\frac{u(m, n+1, l) - u(m, n, l)}{\Delta z} \right] - \left[\frac{\beta^2(m, n) + \beta^2(m, n-1)}{2} \right] \left[\frac{u(m, n, l) - w(m, n-1, l)}{\Delta z} \right] \right\} \end{aligned}$$

$$\begin{aligned} \frac{w(m, n, l+1)}{\Delta t^2} &= \frac{2w(m, n, l) - w(m, n, l-1)}{\Delta t^2} + \frac{1}{2\Delta z} \{ \alpha^2(m, n+1) \left[\frac{u(m+1, n+1, l) - u(m-1, n+1, l)}{2\Delta x} \right] - \\ &\quad \alpha^2(m, n-1) \left[\frac{u(m+1, n-1, l) - u(m-1, n-1, l)}{2\Delta x} \right] \} + \frac{1}{\Delta z} \left\{ \left[\frac{\alpha^2(m, n+1) + \alpha^2(m, n)}{2} \right] \right. \\ &\quad \left. \left[\frac{w(m, n+1, l) - w(m, n, l)}{\Delta z} \right] - \left[\frac{\alpha^2(m, n) + \alpha^2(m, n-1)}{2} \right] \left[\frac{w(m, n, l) - w(m, n-1, l)}{\Delta z} \right] \right\} \\ &\quad + \frac{2}{2\Delta z} \{ \beta^2(m, n+1) \left[\frac{u(m+1, n+1, l) - u(m-1, n+1, l)}{2\Delta x} \right] - \beta^2(m, n-1) \\ &\quad \left[\frac{u(m+1, n-1, l) - u(m-1, n-1, l)}{2\Delta x} \right] \} + \frac{1}{\Delta x} \left\{ \left[\frac{\beta^2(m+1, n) + \beta^2(m, n)}{2} \right] \right. \\ &\quad \left. \left[\frac{w(m+1, n, l) - w(m, n, l)}{\Delta x} \right] - \left[\frac{\beta^2(m, n) + \beta^2(m-1, n)}{2} \right] \left[\frac{w(m, n, l) - w(m-1, n, l)}{\Delta x} \right] \right\} + \\ &\quad + \frac{1}{2\Delta x} \{ \beta^2(m+1, n) \left[\frac{u(m+1, n+1, l) + u(m+1, n-1, l)}{2\Delta z} \right] \right. \\ &\quad \left. - \beta^2(m-1, n) \left[\frac{u(m-1, n+1, l) - u(m-1, n-1, l)}{2\Delta z} \right] \right\} \end{aligned} \quad (2)$$

SOURCE FUNCTIONS

A number of source wavelets are in use in seismic data processing with well-studied frequency and time domain characteristics. Model stability is found to be directly related with the nature of seismic source. Model stability and effects like numerical anisotropy is also found time dependent.

DIRAC OR SPIKE WAVELET

The spike or a unit impulse is the simplest most wavelet. It is represented by a Dirac delta function $\delta(t)$ mathematically,

$$\delta(t) = \begin{cases} 1 & t = 0 \\ 0 & t \neq 0 \end{cases}$$

The Fourier transform of Dirac delta has unit amplitude for all frequencies $-\pi \leq \omega \leq \pi$, which shows that Dirac pulse

has white spectrum. In FDM modeling, the Dirac impulse may produce grid dispersion due to its broad spectrum.

EXPLOSIVE POINT SOURCE

This source is commonly employed in the reflectivity method, e.g. Fertig and Muller (1978) and Fuchs and Muller (1971). Shtivelman (1984) has also used this source for preparation of the synthetic seismograms by hybrid method. The hybrid method devised by him combines FDM and ray scheme.

The relation below gives the time variation of excitation function,

$$f(t) = \begin{cases} \sin \delta t - 1/m \sin m \delta t & 0 \leq t \leq T \\ 0 & t < 0 \text{ \& } t > T \end{cases}$$

where $\delta = N\pi / T$, $m = (N+2) / N$, $N = 1, 2, 3, \dots$

Input parameters required to generate the wavelet are the time duration T and the number N of extrema in the interval $(0, T)$. A number of different signals can be generated from a single excitation function by changing the values of above parameters. The time variation of the source has a component of characteristic *sinc* function of the type Sinx/x . The signal in figure 1 is generated by using the $N = 2$ and $T = 30 \text{ m sec}$. The frequency spectrum of the source shows that it is centered about the frequency of 50 Hz and has another component of relatively smaller magnitude centered about 110 Hz. But any component above the 100 Hz can be neglected and 100 Hz can be taken as the highest component of frequencies contained in the signal. The increment time of our computations is 2 m sec, which corresponds to a Nyquist frequency of 250 Hz.

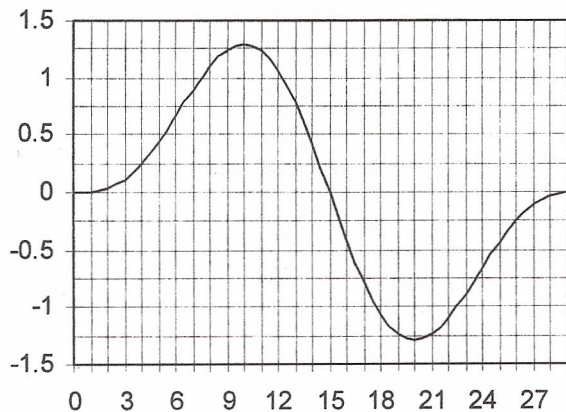


Figure 1- Time variation of Explosive Source Function.

GABOR WAVELET

This wavelet is close to the physical wavelets and does not involve the Gibb's effect that appears as the result of artificial truncation of signal in *sinc* functions such as described by Pan (1998). It can produce signal whose main or dominant frequency can be controlled as an initial parameter (Hubral and Tygel, 1989). The real part of such

wavelets (cosine wavelet) is a zero phase wavelet symmetric in the time domain. The imaginary part (sine wavelet) is anti symmetric and is in quadrature with the corresponding cosine wavelet. According to Morlet et al. (1982) the Gabor wavelet is defined as,

$$g(t) = e^{-\left(\frac{2t}{\Delta t}\right)^2 \ln 2} e^{i\omega_0 t}$$

While writing the above equation, we have taken zero as origin time and maximum amplitude is normalized to 1. The two parameters ω_0 and Δt are the mean angular frequency and the duration or diameter defined as the time interval separating the two points on the envelope where the modulus drops to 1/2. The signal in figure 2 is generated by using $\Delta t = 40 \text{ m sec}$ and $f = 50 \text{ Hz}$.

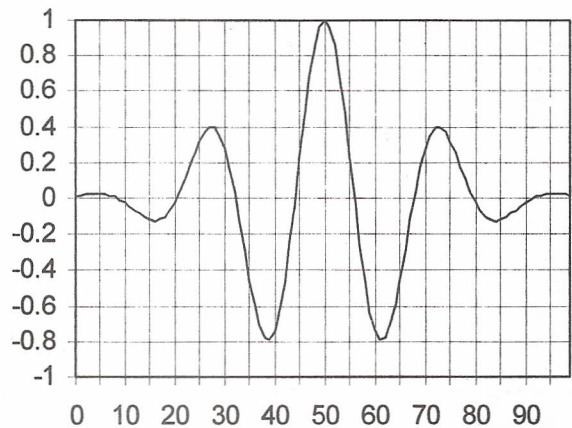


Figure 2- Time variation of a Gabor Wavelet.

RICKER WAVELET

This is one of the earliest developed and well studied (Longman, 1980) and most widely used mathematical source. It has similar time variation as of the source used by Seron et al. (1996) in numerical modeling. The time variation of the source based on Ricker wavelet is shown in the figure 3. The mathematical function governing the Ricker wavelet is given by Sherif and Geldart, (1993),

$$f(t) = \left(1 - 2\pi^2 f_p^2 t^2\right) e^{-\pi^2 f_p^2 t^2}$$

Where f_p is the central frequency of the signal. The source frequency in present study is kept at 20 Hz.

MINIMUM PHASE WAVELET

The minimum phase wavelet has its energy loaded at its front part. This source function approximates the dynamite source used in field. The time amplitude graph of the minimum phase wavelet is shown in figure 4. The source function for the generation of minimum phase wavelet is,

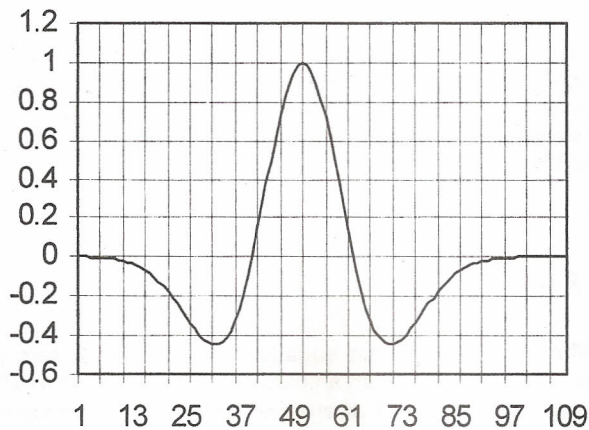


Figure 3- Time variation of Ricker wavelet.

Where A is the maximum amplitude and f is the central

$$g(t) = -A(\sin(2\pi ft))e^{-\pi t^2}$$

frequency of the wavelet. The amplitude units are arbitrary and are different from those used in modeling.

THE MODELING PROCEDURE

We have discussed the modeling results of amplitude anomaly model by Kelly et al. (1976) with different source wavelet functions. The Poisson's ratio of $1/\sqrt{2}$ is maintained throughout the model. For the lower values of Poisson's ratio, the S-waves generated at interfaces travel with lower velocities, resulting in wavelengths much smaller than P-waves of the similar frequency. This causes grid dispersion, which leads to system instability. The attempt to overcome this effect by decreasing the node spacing has three major drawbacks. First it increases the number of required node points, second the source amplitude must have low value so that the gradients are small enough for the system stability, and finally the time step must be decreased in order to satisfy the conditions of the system stability. Even under the conditions of constant Poisson's ratio of $1/\sqrt{2}$, grid dispersion some times appears in the resulting data. This effect is suppressed by frequency filtering the synthetic seismograms for high frequencies producing grid dispersion. The idea of getting rid of grid dispersion by frequency filtering is not new; Smith (1975) has used this technique in Finite Element Method (FEM) modeling. The Automatic Gain Control (AGC) with a window of 100 m sec to compensate for the dispersive losses is applied. It has also been done by Reshef et al. (1988 a, b) who have applied AGC on synthetic seismograms prepared by 3D acoustic and elastic modeling using the Fourier method. The models discussed are same in dimensions as discussed by the Kelly et al. (1976).

The model outputs using Gabor and Dirac Delta functions are dominated by grid dispersion and as its effect could not be removed by frequency filtering so they are not discussed here.

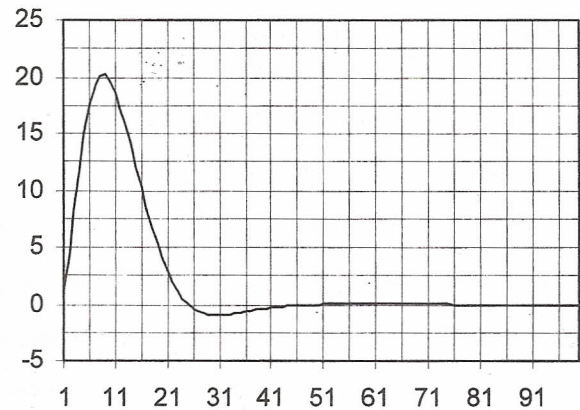


Figure 4- Time variation of minimum phase wavelet

THE MODEL

The model consists of three layers (Figure 5). The top most layer has P-wave velocity of 7100 ft/sec. The source is exploded at a depth of 380 ft. The first interface is at a depth of 1180 ft. The second layer P-wave velocity is 6900 ft/sec. Second interface is at 1280 ft with lower layer having P-wave velocity of first layer i.e. 7100 ft/sec. All above sources are used for the same model specification.

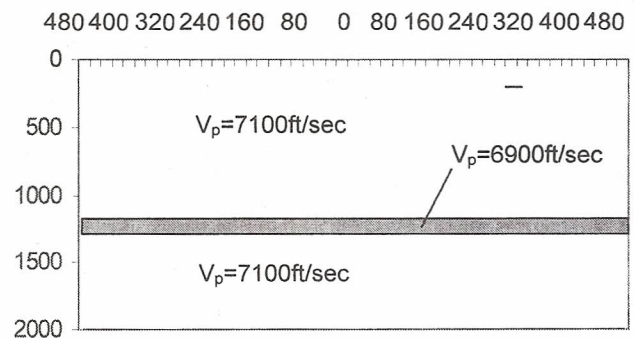


Figure 5- The model geometry.

As a part of processing, instantaneous or Root Mean Square AGC is applied with a time window of 100 m sec (unless otherwise mentioned). The results for all sources are discussed separately in following sections:

Model Response of Explosive Source

The synthetic seismograms prepared by using the explosive point source have many advantages over the Dirac pulse. This source provides control over the frequency of the input signal, that can help in reducing the grid dispersion and related phenomenon. The shape of impulsive source used contains two peaks and frequency filtering has almost no such effects as shape modification. The model response of impulsive source is first applied with AGC and then is convolved with band pass filter of window 10-40 Hz. AGC is again applied to get results. As apparent in the figure 6, the synthetic seismograms prepared by using the explosive source are usable up to the last part of

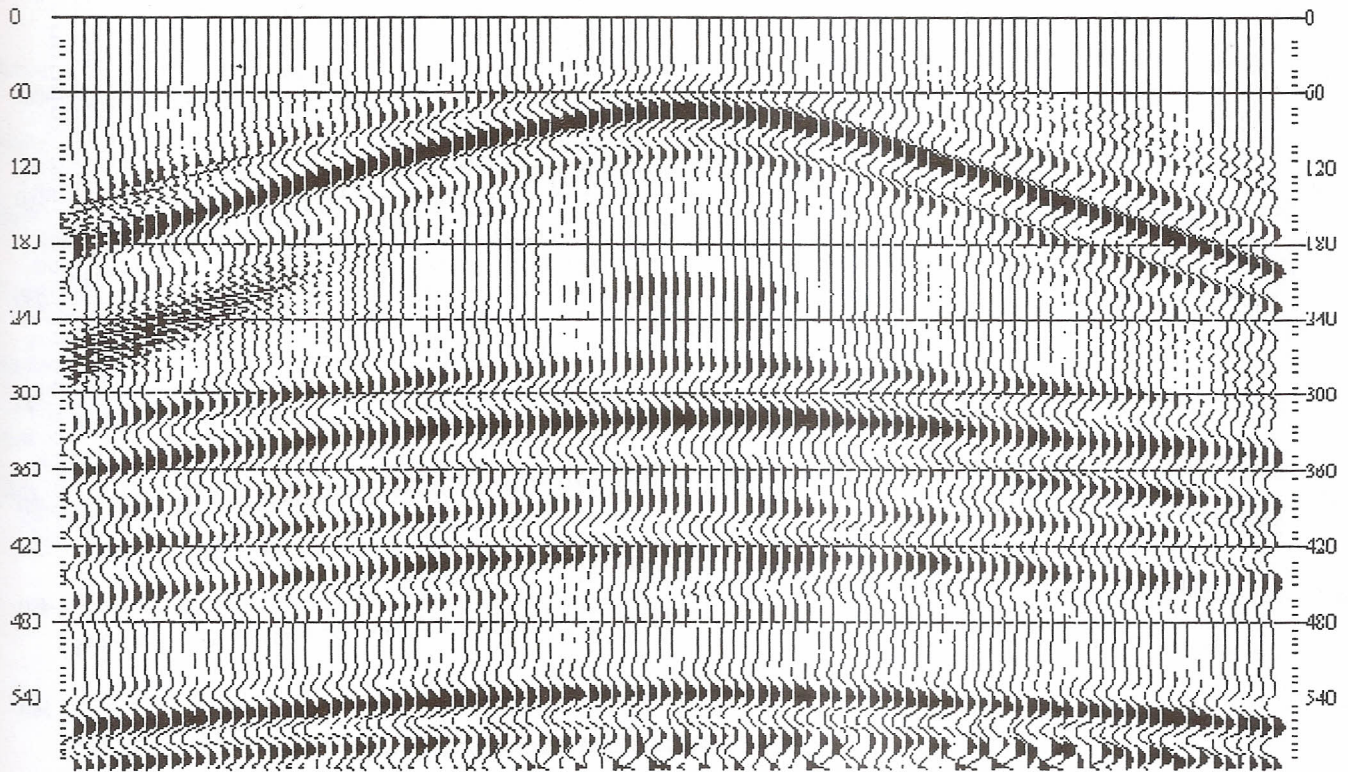


Figure 6- CSP gather prepared by using explosive point source.

section. The arrival times of the reflection events are similar in both cases. The Common Shot Point (CSP) gather prepared by this source also shows numerical anisotropy in the upper parts of the section but in lower parts the response is almost symmetric.

Model Response of Ricker Wavelet

The model is observed to be stable for the velocity distribution model of Kelly et al. (1976) for source frequency of 20 Hz. The shape of Ricker wavelet involves gradual build up and decay of energy (Figure 3), this increases the formulation stability. The Ricker wavelet does not seem to be susceptible to FDM anisotropy (Figure 7) so it travels through the grid with maximum symmetry, CSP gather appears to be completely symmetric across the shot point. The arrival times appearing on the seismic section are similar to that of Kelly et al. (1976). Processing on Ricker wavelet response is also simple and consists of applying AGC gain, and convolution with Ricker wavelet of the same frequency as that of the source.

Model Response of Minimum Phase Wavelet

Common shot point gather prepared by using the minimum phase wavelet with frequency centered about 20 Hz (Figure 8) shows model to be stable. No grid dispersion is visible on the final gather. The processing for the minimum phase wavelet is similar to the Ricker wavelet and involves convolution of the model out put with minimum phase wavelet of same as source frequency. The numerical anisotropy that is apparent in the initial part of gather decreases with increasing time.

CONCLUSIONS

The attempt to overcome the grid dispersion and related phenomenon by frequency filtering is successful only if the system instability is within certain limits.

The model stability although mainly influenced by the dominant frequency of the signal is also dependent on the phase characteristics of the source function.

The numerical anisotropy in all the model prepared with different source functions decays with time.

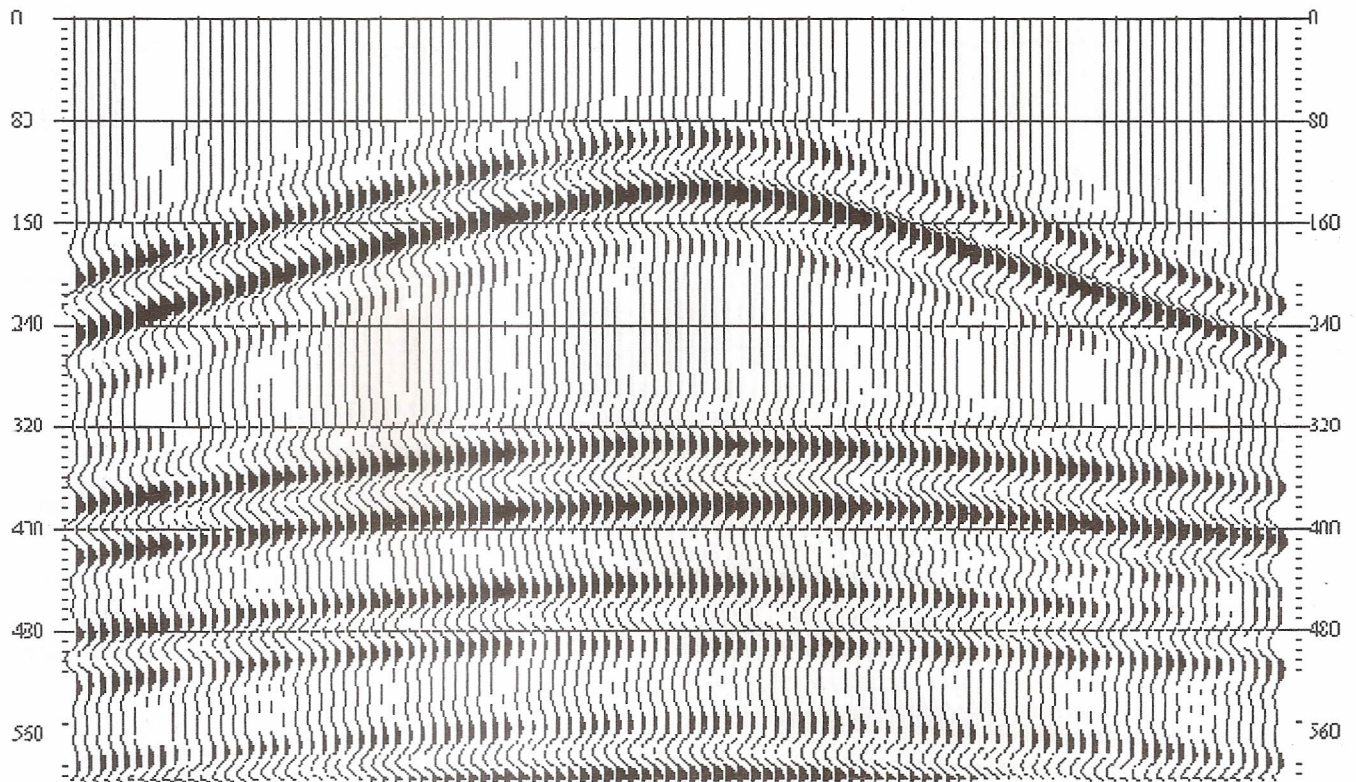


Figure 7- CSP gather prepared by using Ricker wavelet source.



Figure 8- CSP gather prepared by using Minimum phase wavelet source.

REFERENCES

- Alford, R. M., K.R. Kelly and D.M. Boore, 1974, Accuracy of finite-difference modeling of the acoustic wave equation: *Geophys.* v.39, no.6, p.834-842.
- Fertig, J. and G. Muller, 1978, Computation of synthetic seismograms for coal seams with the reflectivity method: *Geophys. Pros.* 26, p.868-883.
- Fuchs, K. and G. Muller, 1971, Computation of synthetic seismograms with the reflectivity method and comparison with observations: *Geophys. J. Roy. astr. Soc.* 23, p.417-433.
- Fornberg, B., 1987, The pseudospectral method: Comparison with finite differences for the elastic wave equation: *Geophys.* 52, p.483-501.
- Huatao W. U. and J.M. Lees, 1997, Boundary conditions on a finite grid: Applications with pseudospectral wave propagation: *Geophys.*, v.62, no.5, p.1544-1557.
- Hubral, P. and M. Tygel, 1989, Analysis of the Rayleigh pulse: *Geophys.*, v.54, no.5, p.654-658.
- Kelly, K. R., R.W. Ward, S. Treitel and R.M. Alford, 1976, Synthetic seismograms: A Finite Difference Approach: *Geophys.*, v.41, no.1, p.2-27.
- Longman, M.I., 1980, The calculation of seismic wavelet functions: *Geophys.*, v.45, no.6, p.1055-1060.
- Morlet, L., G. Arens, E. Fourgeau and D. Giard, 1982, Wave propagation and sampling theory-part 2: Sampling theory and complex wave: *Geophys.*, v.47, no.2, p.222-236.
- Pan, C., 1998, Spectral ringing suppression and optimal windowing for attenuation and Q measurements: *Geophys.*, v.63, no.2, p.632-636.
- Randall, C. J., 1988, Absorbing boundary condition for the elastic wave equation: *Geophys.*, v.53, no.5, p.611-624
- Reshef, M., D. Kosloff, M. Edwards and C. Hsiung, 1988, Three dimensional acoustic modeling by the Fourier method: *Geophys.*, v.53, no.9, p.1175-1183.
- Seron, F. J., J. Badal and F.J. Sabadell, 1996, A numerical laboratory for simulation and visualization of seismic wavefields: *Geophys. Pros.* 44, p.603-642.
- Sherif, R.E., and L.P. Geldart, 1993, *Exploration Seismology*. v.1, Cambridge Univ. Press.
- Shtivelman, V., 1984, A hybrid method for wave field computation: *Geophys. Pros.* 32, p.236-257.
- Wild, A.J. and S.C. Singh, 1998, Some unintended features of elastic finite-difference models: *Geophys. Pros.* 46, p.79-101.